DNA Bending through Roll Angles Is Independent of Adjacent Base Pairs

ARTICLE *in* JOURNAL OF PHYSICAL CHEMISTRY LETTERS · OCTOBER 2012

Impact Factor: 7.46 · DOI: 10.1021/jz301227y

THE JOURNAL OF PHYSICAL CHEMISTRY Letters

Letter

pubs.acs.org/JPCL

DNA Bending through Roll Angles Is Independent of Adjacent Base Pairs

Justin Spiriti and Arjan van der Vaart*

Department of Chemistry, University of South Florida, 4202 East Fowler Avenue CHE 205, Tampa, Florida 33620, United States

Supporting Information

ABSTRACT: We have studied DNA bending for a wide range of DNA sequences by two-dimensional adaptive umbrella sampling simulations on adjacent roll angles. Calculated free energy surfaces are largely additive and can be well approximated by the sum of the one-dimensional free energy surfaces. Cooperativity between adjacent roll angles was found to be negligible: less than 1.0 kcal/mol and a small fraction of the overall bending energy. Our calculations validate the assumptions underlying many popular coarse-grained models for DNA bending, and demonstrate their theoretical validity for investigating DNA bending.

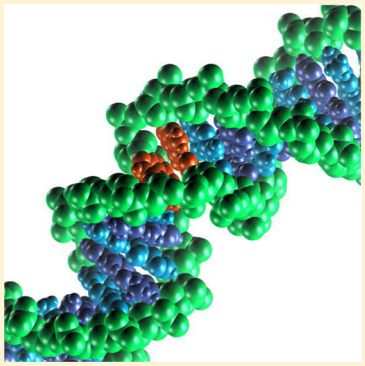

SECTION: Biophysical Chemistry and Biomolecules

DNA undergoes many large scale conformational changes as part of its biological function. These include being bent and wrapped around packaging proteins in prokaryotes and histones in eukaryotes,[1−3] and being bent or kinked by a variety of gene regulatory proteins.[4] DNA bending makes an important contribution to the thermodynamics of protein−DNA binding. In proteins that bend the DNA significantly, the unfavorable enthalpic contribution to binding due to the destacking of bases and increased phosphate repulsion is offset by favorable entropic contributions from water release and configurational entropy of the protein;[5] molecular dynamics (MD) simulations of the *lac* repressor headpiece show that these factors determine the equilibrium bending angle.[6] In proteins that do not bend the DNA significantly, a coupled protein folding process often provides an unfavorable entropic contribution that modulates the binding affinity.[5,7]

Due to its stiffness, DNA bending takes place on time scales larger than those that can be easily studied using unbiased atomistic MD simulations. This problem can be overcome by enhancing the sampling using techniques such as umbrella sampling,[8−11] which can sample the important conformations within time scales accessible to MD. Alternatively, coarse-grained modes for DNA can be used in which each particle represents more than one atom. Many such models have been constructed, varying in the level of detail from multiple particles per nucleotide[12−16] to one particle per base pair.[17−23]

In the latter approach, linear response theory is used to relate the large scale physical properties of DNA to fluctuations in the base pair step parameters. The assumption is made that correlations between base pairs that are not nearest neighbors can be neglected,[20−23] in contrast with the well-known cooperative nature of the helix−coil transition in proteins.[24,25] Alternatively, several models feature van der Waals interactions between bases,[14,26] but interactions between bases in the same or neighboring base pair step dominate over those more distant. Some recent studies suggest that long-range correlations in geometrical properties along the DNA might be important. For example, analysis of curvature fluctuations from DNA shows that the Hurst exponent of the curvature fluctuations of human DNA is larger than the corresponding Hurst exponent for hepatitis C viral DNA, indicating long-range correlations in the human DNA but not in the viral DNA;[27,28] similar long-range correlations are seen in the sequence and may reflect nucleosome positioning patterns.[29] It is possible that these correlations could have a significant influence on DNA structure and dynamics, which would invalidate coarse grained models which assume that such correlations can be neglected.

Thus far, no physical basis for this assumption exists. In order to determine whether certain long-range correlations in DNA can be neglected in coarse-grained models for DNA bending, we carried out atomistic free energy simulations of DNA bending. Statistical studies showed that DNA bending primarily occurs through changes in the roll angle.[30] We therefore enhanced the sampling of the roll angle in our simulations; to assess cooperativity, we performed two-dimensional adaptive umbrella sampling on adjacent roll angles and subtracted one-dimensional free energies from the resultant surfaces.

Received: August 21, 2012
Accepted: October 3, 2012
Published: October 3, 2012

Table 1. Sequences Simluated and Convergence of Free Energy Surfaces

name	sequence[a]	number of iterations[b]	maximum absolute difference between free energy surfaces (kcal/mol)[c]		
GACGT[d]	5′-CGCG**ACG**TCGCG-3′	80	0.075	0.113	0.047
GATGT[d]	5′-CGCG**ATG**TCGCG-3′	80	0.055	0.056	0.042
GAAAT[d]	5′-CGCG**AAA**TCGCG-3′	80	0.072	0.048	0.052
GTAAA[d]	5′-CGCG**TAA**ACGCG-3′	80	0.058	0.090	0.043
GATAT	5′-CGCG**ATA**TCGCG-3′	80	0.058	0.104	0.063
GTCGA	5′-CGCG**TCG**ACGCG-3′	80	0.047	0.073	0.037
GCGAG	5′-CGCG**CGA**GCGCG-3′	90	0.096	0.044	0.120
GTATA	5′-CGCG**TAT**ACGCG-3′	90	0.170	0.058	0.074
ATATC	5′-CGCA**TAT**CGCG-3′	80	0.048	0.195	0.183
TCGAC	5′-CGCT**CGA**CGCG-3′	80	0.170	0.040	0.050
TAATT	5′-CGCT**AAT**TGCG-3′	80	0.064	0.059	0.061
TTAAC	5′-CGCT**TAA**CGCG-3′	80	0.085	0.040	0.141
CGAGT	5′-CGCC**GAG**TGCG-3′	80	0.076	0.079	0.138
GCGCC	5′-CGCG**CGC**CGCG-3′	80	0.219	0.139	0.251

[a]Base pairs subjected to umbrella sampling are shown in bold for each sequence. [b]500 ps per iteration. [c]Shown for last the three iterations of adaptive umbrella sampling, and calculated on the part of the free energy surface below the biasing cap. [d]Used as control.

Table 1 lists the simulated DNA sequences. Four 12-mers were constructed by selecting central base pair trimers which showed significant bending in a set of 490 unique protein−DNA crystal structures listed in ref 31; another four did not show significant bending in crystal structures and were used as controls. Each of the trimers was embedded in the 5′-CGCGN$_1$N$_2$N$_3$N$_4$CGCG-3′ sequence, where N$_1$N$_2$N$_3$ equals the trimer and N$_4$ is complementary to N$_1$. Since the average and standard deviation of DNA roll angles are also affected by flanking base pairs,[32−34] six more sequences were chosen in which the central pentamer was varied. These sequences have diverse flanking residues, and are well represented in the protein−DNA crystal structures, with a substantial fraction of the crystal structures showing significant bending. These sequences were embedded in the standard sequence 5′-CGCNNNNNGCG-3′ to form 11-mers. Clearly, our selection of structures merely represents a subset of possible structures. Due to the large computational expense, it was not possible to simulate each of the 32 possible trimers or 512 possible pentamers. Consequently, only a selection of trimers or pentamers could be studied. We made this selection judiciously, choosing sequences that show large bending in protein−DNA crystal structures as well as a number of controls that did not show significant bending.

Initial coordinates representing B-form DNA were constructed for each sequence using 3DNA,[19] after which each system was minimized, solvated in a rhombic dodecahedral box with 150 mM KCl and explicit water[35] extending at least 12 Å from the DNA, heated, and equilibrated. The free energy surface of DNA bending in terms of the roll angles was determined by two-dimensional adaptive umbrella sampling using the pseudoroll angle[31] as a reaction coordinate. In contrast to the roll angle, the pseudoroll angle definition does not need an idealized base pair reference frame; therefore, calculation of the pseudoroll angle and its derivatives is much less costly. The pseudoroll angle was previously shown to have a perfect correlation with the true roll angle;[31] a diagram illustrating the coordinate is shown in the Supporting Information. Two-dimensional histograms of the pseudoroll angle were calculated with a bin size of 5°, and the potential of mean force was recalculated every 500 ps using the weighted histogram analysis method[36] until convergence, for a total production length of 40 or 45 ns (Table 1). Since the (pseudo)roll angle is ill-defined when bases flip, a cap on the biasing potential was imposed to prevent base flipping, a high energy process.[31] The biasing cap limits the energy range of the sampling; this also means that while simulations can converge below the cap, no convergence can be obtained beyond. The caps were found in an iterative way, starting from high caps and lowering the caps if base flipping started to occur. The resulting caps were 10 kcal/mol for the dodecamers, 9.5 kcal/mol for all 11-mers except TTACC, and 9.0 kcal/mol for the TTACC 11-mer. All simulations used the particle mesh Ewald method,[37] a time step of 2 fs, and SHAKE constraints,[38] and were carried out in the NPT ensemble using the Nosé-Hoover method.[39] All simulations were performed using an in-house modified version of CHARMM,[31,40] using the AMBER parambsc0 force field.[41]

In order to determine the implied means $\bar{\rho}$ and standard deviations σ of the roll angles whose sampling was enhanced, the portion of the free energy surface below 3 kcal/mol was fitted to:

$$F(\rho_5, \rho_6) = a_5(\rho_5 - \bar{\rho}_5)^2 + a_6(\rho_6 - \bar{\rho}_6)^2 + F_0 \quad (1)$$

A value of 3 kcal/mol was used in order to enable accurate comparisons with ABC consortium data,[34] which does not include as highly bent structures. Here the roll angles are normally distributed, and the coefficients a_i follow from $\sigma^2 = kT/(2a_i)$. In order to account for the possibility of correlation between the adjacent roll angles, a similar fit was performed with a cross term:

$$F(\rho_5, \rho_6) = a_5(\rho_5 - \bar{\rho}_5)^2 + a_6(\rho_6 - \bar{\rho}_6)^2 + b(\rho_5 - \bar{\rho}_5)(\rho_6 - \bar{\rho}_6) + F_0 \quad (2)$$

In this case the roll angles follow a bivariate normal distribution with a correlation coefficient of $r = 2b/(a_5a_6)^{1/2}$.

Cooperativity in DNA bending was calculated by subtracting the one-dimensional free energy surfaces for each of the roll angles from the two-dimensional free energy surfaces. The one-dimensional free energy surfaces were obtained by numerical integration of the two-dimensional surfaces. The free energy of cooperativity is negative if DNA bending through roll angles is cooperative, and positive if the bending is anticooperative. The calculated free energy of cooperativity values were subsequently

dx.doi.org/10.1021/jz301227y | J. Phys. Chem. Lett. 2012, 3, 3029−3033

used to assess roll angle cooperativity in the database of unique protein−DNA structures from ref 31. Because the distribution of base pair step parameters is affected by the identity of flanking base pairs,[32−34] only sequences with pentamers that matched the pentamer in the simulated DNA sequences were considered. To ease the interpretation of the data, estimated free energies of cooperativity for these structures were plotted against the degree of distortion $\chi = (\rho_5^2 + \rho_6^2)^{1/2}$.

To verify that the simulations showed the proper long-range DNA behavior, persistence lengths were calculated from the simulation data.[31,42] Despite the fact that these persistence lengths were extrapolated from short-length simulations, calculated values were consistent with previous simulations and experiments (see Supporting Information).

Table 1 shows the maximum absolute difference between the free energy surfaces below the biasing cap on successive adaptive umbrella runs. Judging from the table, the simulations were well converged below the cap. This part of the free energy surface extended to roll angles of approximately ±45° in each direction, and included highly bent DNA structures (for comparison, the roll angles vary between −27° and 24° in the nucleosome[2]).

Contour plots of the two-dimensional free energy surfaces in terms of roll angles are shown in Supporting Information, as well as the one-dimensional free energy surfaces obtained from numerical integration. The two-dimensional free energy surfaces are largely additive in terms of the one-dimensional free energy surfaces, as indicated by the shapes of the contours. Contour plots of the free energy of cooperativity (Figure 1)

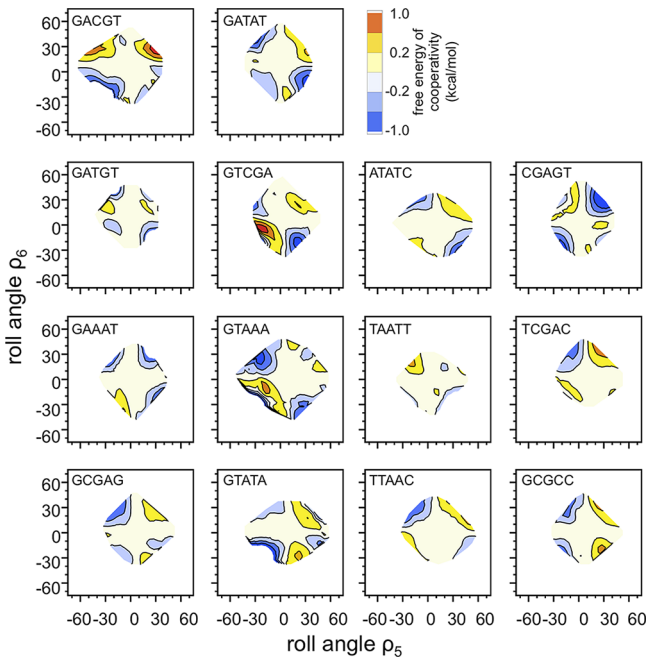

Figure 1. Free energy of cooperativity, shown for areas for which the two-dimensional free energy is less than the biasing cap.

demonstrate that below the biasing cap the cooperativity is generally less than 0.6 kcal/mol in magnitude. For a few sequences, small areas of higher cooperativity (up to 1 kcal/mol) are encountered, for example for GACGT, GTCGA, and CGAGT. These areas are at extreme bending angles, at the border of the converged areas (that is, the corresponding two-dimensional free energy surface is near the biasing cap). Consequently, the free energies of cooperativity are small compared to the overall bending free energy.

The means and standard deviations of the roll angles, obtained by assuming independent roll angles and fitting the two-dimensional free energy surfaces to eq 1, are very similar to the values observed previously (Supporting Information). In particular, pyrimidine-purine base pair steps have a positive equilibrium roll angle of about 10° and increased flexibility, as observed in other simulations[31,34] and surveys of DNA crystal structures.[20] In addition, there is a variation of approximately 2−5° in the mean value and about 1° in the standard deviation due to sequence context, which was also observed by the ABC consortium.[34] Fitting the surfaces to eq 2, which includes a cross term to account for correlations between the two roll angles, showed that the cross term is statistically significant in only five out of 14 cases (GTCGA, GCGAG, TCGAC, CGAGT and GCGCC). In these cases, the degree of correlation between roll angles is modest, with the implied correlation coefficient r ranging from approximately 0.2 to 0.4. This is another confirmation that there is generally little cooperativity or correlation between adjacent roll angles.

Figure 2 shows the relationship between the free energy of cooperativity and distortion for pentamers taken from the

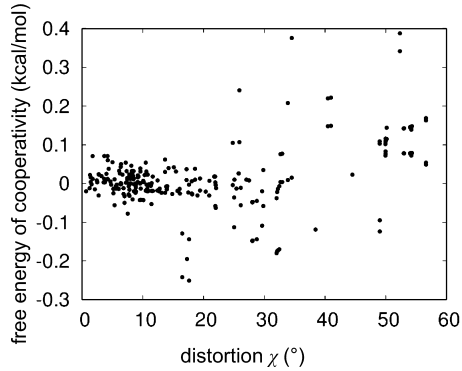

Figure 2. Scatterplot of the free energy of cooperativity as a function of distortion in the central two base pair steps of DNA pentamers taken from the protein−DNA crystal structure database. Shown for points for which the two-dimensional free energy is less than the biasing cap.

protein−DNA crystal structure database. The magnitude of the cooperativity increases with increasing distortion, although, even for protein−DNA complexes with highly distorted DNA, this cooperativity does not exceed 0.4 kcal/mol in absolute value. In addition, there does not appear to be a bias toward positive or negative values of the cooperativity in protein−DNA crystal structures.

Our data demonstrates that there is little cooperativity between adjacent roll angles in DNA. Cooperativity in DNA bending is generally less than 0.6 kcal/mol, and no more than 1 kcal/mol, an order of magnitude less than the overall free energy cost of bending DNA through large angles. This lack of cooperativity is consistent with the ABC consortium simulations, which found only weak effects of flanking sequence on tilt and roll.[34] It is also consistent with stacking of bases being the more important force contributing to DNA flexibility for small bending angles, since quantum calculations indicate that base stacking is primarily a dispersion force and is consequently short-ranged.[43] The results suggest that protein−DNA binding affinities are unaffected by cooperativity in DNA bending. This

dx.doi.org/10.1021/jz301227y | J. Phys. Chem. Lett. 2012, 3, 3029−3033

means that concerted mechanisms to kink DNA at multiple base pair steps are not more or less energetically costly than kinking DNA one base pair step at a time, and may help explain why a protein like the *Escherichia coli* integration host factor bends DNA in a concerted fashion.[44−46]

Because only the roll angle was studied, cooperative fluctuations in other base pair step parameters, such as longitudinal fluctuations,[47] cannot be ruled out. However, since DNA bending is mostly determined by changes in the roll angle,[30] possible correlations in other parameters will likely be less important for the overall structure of DNA. In summary, our calculations show that roll angles are largely independent of one another. The study validates the assumption of independence of adjacent base pairs in popular coarse-grained models for DNA bending,[20−23] strengthening the theoretical justification of such models.

■ ASSOCIATED CONTENT

Supporting Information

Definition of the pseudoroll angle, the protocol for the calculation of persistence lengths, tables with roll angle statistics and persistence lengths, and figures of two- and one-dimensional free energy surfaces are provided as Supporting Information. This material is available free of charge via the Internet at http://pubs.acs.org.

■ AUTHOR INFORMATION

Corresponding Author

*E-mail: avandervaart@usf.edu; Tel.: 813-974-8762; Fax: 813-974-3203.

Author Contributions

The manuscript was written through contributions of all authors. All authors have given approval to the final version of the manuscript.

Notes

The authors declare no competing financial interest.

■ ACKNOWLEDGMENTS

This work was supported by NSF CAREER award no. CHE-1007816. Computer time was provided by USF Research Computing and XSEDE.

■ ABBREVIATIONS

MD - molecular dynamics; NPT - constant number of particles, pressure and temperature

■ REFERENCES

(1) Luijsterburg, M. S.; White, M. F.; van Driel, R.; Dame, R. T. The Major Architects of Chromatin: Architectural Proteins in Bacteria, Archaea and Eukaryotes. *Crit. Rev. Biochem. Mol. Biol.* **2008**, *43*, 393−418.

(2) Richmond, T. J.; Davey, C. A. The Structure of DNA in the Nucleosome Core. *Nature* **2003**, *423*, 145−150.

(3) Gurunathan, K.; Levitus, M. Single-Molecule Fluorescence Studies of Nucleosome Dynamics. *Curr. Pharm. Biotechnol.* **2009**, *10*, 559−568.

(4) Allemann, R. K.; Egli, M. DNA Recognition and Bending. *Chem. Biol.* **1997**, *4*, 643−650.

(5) Jen-Jacobson, L.; Engler, L. E.; Jacobson, L. A. Structural and Thermodynamic Strategies for Site-Specific DNA Binding Proteins. *Structure* **2000**, *8*, 1015−1023.

(6) Barr, D.; van der Vaart, A. The Natural DNA Bending Angle in the Lac Repressor Headpiece-O1 Operator Complex Is Determined by Protein-DNA Contacts and Water Release. *Phys. Chem. Chem. Phys.* **2012**, *14*, 2070−2077.

(7) Spolar, R. S.; Record, M. T. Coupling of Local Folding to Site-Specific Binding of Proteins to DNA. *Science* **1994**, *263*, 777−784.

(8) Torrie, G. M.; Valleau, J. P. Non-Physical Sampling Distributions in Monte-Carlo Free-Energy Estimation - Umbrella Sampling. *J. Comput. Phys.* **1977**, *23*, 187−199.

(9) Hooft, R. W. W.; Vaneijck, B. P.; Kroon, J. An Adaptive Umbrella Sampling Procedure in Conformational-Analysis Using Molecular-Dynamics and Its Application to Glycol. *J. Chem. Phys.* **1992**, *97*, 6690−6694.

(10) Bartels, C.; Karplus, M. Multidimensional Adaptive Umbrella Sampling: Applications to Main Chain and Side Chain Peptide Conformations. *J. Comput. Chem.* **1997**, *18*, 1450−1462.

(11) Spiriti, J.; Kamberaj, H.; van der Vaart, A. Development and Application of Enhanced Sampling Techniques to Simulate the Long-Time Scale Dynamics of Biomolecular Systems. *Int. J. Quantum Chem.* **2012**, *112*, 33−43.

(12) Knotts, T. A.; Schwartz, D. C.; de Pablo, J. J. A Coarse Grain Model for DNA. *J. Chem. Phys.* **2007**, *126*, 084901.

(13) Dans, P. D.; Zeida, A.; Pantano, S. A Coarse Grained Model for Atomic-Detailed DNA Simulations with Explicit Electrostatics. *J. Chem. Theory Comput.* **2010**, *6*, 1711−1725.

(14) Morriss-Andrews, A.; Rottler, J.; Plotkin, S. S. A Systematically Coarse-Grained Model for DNA and Its Predictions for Persistence Length, Stacking, Twist, and Chirality. *J. Chem. Phys.* **2010**, *132*, 035105.

(15) Ouldridge, T. E.; Louis, A. A.; Doye, J. P. K. DNA Nanotweezers Studied with a Coarse-Grained Model of DNA. *Phys. Rev. Lett.* **2010**, *104*, 178101.

(16) Savelyev, A.; Papoian, G. A. Chemically Accurate Coarse Graining of Double-Stranded DNA. *Proc. Natl. Acad. Sci. U.S.A.* **2010**, *107*, 20340−20345.

(17) Babcock, M. S.; Pendault, E. P. D.; Olson, W. K. Nucleic Acid Structure Analysis: Mathematics for Local Cartesian and Helical Structure Parameters That Are Truly Comparable between Structures. *J. Mol. Biol.* **1994**, *237*, 125−156.

(18) Lu, X.-J.; Olson, W. K. Resolving the Discrepancies among Nucleic Acid Conformational Analyses. *J. Mol. Biol.* **1999**, *285*, 1563−1575.

(19) Lu, X.-J.; Olson, W. K. 3DNA: A Software Package for the Analysis, Rebuilding and Visualization of Three-Dimensional Nucleic Acid Structures. *Nucleic Acids Res.* **2003**, *31*, 5108−5121.

(20) Olson, W. K.; Gorin, A. A.; Lu, X.-J.; Hock, L. M.; Zhurkin, V. B. DNA Sequence-Dependent Deformability Deduced from Protein-DNA Crystal Complexes. *Proc. Natl. Acad. Sci. U.S.A.* **1998**, *95*, 11163−11168.

(21) Mergell, B.; Ejtehadi, M.; Everaers, R. Modeling DNA Structure, Elasticity, and Deformations at the Base-Pair Level. *Phys. Rev. E: Stat. Phys., Plasmas, Fluids* **2003**, *68*, 021911.

(22) Olson, W. K.; Colasanti, A. V.; Czapla, L.; Zheng, G. Insights into the Sequence-Dependent Macromolecular Properties of DNA from Base-Pair Level Modeling. In *Coarse-Graining of Condensed Phase and Biomolecular Systems*; Voth, G. A., Ed.; Taylor & Francis Group: Boca Raton, FL, 209; pp 205−223.

(23) Zhang, Y.; Crothers, D. M. Statistical Mechanics of Sequence-Dependent Circular DNA and Its Application for DNA Cyclization. *Biophys. J.* **2003**, *84*, 136−153.

(24) Schellman, J. A. The Factors Affecting the Stability of Hydrogen-Bonded Polypeptide Structures in Solution. *J. Chem. Phys.* **1958**, *62*, 1485−1494.

(25) Zimm, B. H.; Bragg, J. Theory of the Phase Transition Between Helix and Random Coil in Polypeptide Chains. *J. Chem. Phys.* **1959**, *31*, 526−535.

(26) de Vries, R. Influence of Mobile DNA-Protein-DNA Bridges on DNA Configurations: Coarse-Grained Monte-Carlo Simulations. *J. Chem. Phys.* **2011**, *135*, 125104.

(27) Moukhtar, J.; Fontaine, E.; Faivre-Moskalenko, C.; Arneodo, A. Probing Persistence in DNA Curvature Properties with Atomic Force Microscopy. *Phys. Rev. Lett.* **2007**, *98*, 178101.
(28) Moukhtar, J.; Faivre-Moskalenko, C.; Milani, P.; Audit, B.; Vaillant, C.; Fontaine, E.; Mongelard, F.; Lavorel, G.; St-Jean, P.; Bouvet, P.; et al. Effect of Genomic Long-Range Correlations on DNA Persistence Length: From Theory to Single Molecule Experiments. *J. Phys. Chem. B* **2010**, *114*, 5125−5143.
(29) Audit, B.; Vaillant, C.; Arneodo, A.; d'Aubenton-Carafa, Y.; Thermes, C. Long-Range Correlations between DNA Bending Sites: Relation to the Structure and Dynamics of Nucleosomes. *J. Mol. Biol.* **2002**, *316*, 903−918.
(30) Dickerson, R. E. DNA Bending: The Prevalence of Kinkiness and the Virtues of Normality. *Nucleic Acids Res.* **1998**, *26*, 1906−1926.
(31) Spiriti, J.; Kamberaj, H.; De Graff, A. M. R.; Thorpe, M. F.; van der Vaart, A. DNA Bending through Large Angles Is Aided by Ionic Screening. *J. Chem. Theory Comput.* **2012**, *8*, 2145−2156.
(32) Beveridge, D. L.; Barreiro, G.; Byun, K. S.; Case, D. A.; Cheatham, T. E., III; Dixit, S. B.; Giudice, E.; Lankas, F.; Lavery, R.; Maddocks, J. H.; et al. Molecular Dynamics Simulations of the 136 Unique Tetranucleotide Sequences of DNA Oligonucleotides. I. Research Design and Results on d(CpG) Steps. *Biophys. J.* **2004**, *87*, 3799−3813.
(33) Dixit, S. B.; Beveridge, D. L.; Case, D. A.; Cheatham, T. E., 3rd; Giudice, E.; Lankas, F.; Lavery, R.; Maddocks, J. H.; Osman, R.; Sklenar, H.; et al. Molecular Dynamics Simulations of the 136 Unique Tetranucleotide Sequences of DNA Oligonucleotides. II: Sequence Context Effects on the Dynamical Structures of the 10 Unique Dinucleotide Steps. *Biophys. J.* **2005**, *89*, 3721−3740.
(34) Lavery, R.; Zakrzewska, K.; Beveridge, D.; Bishop, T. C.; Case, D. A.; C., T., III; Dixit, S.; Jarayam, B.; Lankas, F.; Laughton, C.; et al. A Systematic Molecular Dynamics Study of Nearest-Neighbor Effects on Base Pair and Base Pair Step Conformations and Fluctuations in B-DNA. *Nucleic Acids Res.* **2010**, *38*, 299−313.
(35) Jorgensen, W. L.; Chandrasekhar, J.; Madura, J. D.; Impey, R. W.; Klein, M. L. Comparison of Simple Potential Functions for Simulating Liquid Water. *J. Chem. Phys.* **1983**, *79*, 926−935.
(36) Ferrenberg, A. M.; Swendsen, R. H. Optimized Monte Carlo Data Analysis. *Phys. Rev. Lett.* **1989**, *63*, 1195−1198.
(37) Essmann, U.; Perera, L.; Berkowitz, M. L.; Darden, T.; Lee, H.; Pedersen, L. G. A Smooth Particle Mesh Ewald Method. *J. Chem. Phys.* **1995**, *103*, 8577−8593.
(38) Ryckaert, J.-P.; Ciccotti, G.; Berendsen, H. J. C. Numerical Integration of the Cartesian Equations of Motion of a System with Constraints: Molecular Dynamics of *n*-Alkanes. *J. Comput. Phys.* **1977**, *23*, 327−341.
(39) Hoover, W. G. Canonical Dynamics: Equilibrium Phase-Space Distributions. *Phys. Rev. A* **1985**, *31*, 1695−1697.
(40) Brooks, B. R.; Brooks, C. L., III; MacKerell, A. D., Jr.; Nilsson, L.; Petrella, R. J.; Roux, B.; Won, Y.; Archontis, G.; Bartels, C.; Boresch, S.; et al. Charmm: The Biomolecular Simulation Program. *J. Comput. Chem.* **2009**, *30*, 1545−1614.
(41) Perez, A.; Marchan, I.; Svozil, D.; Sponer, J.; C., T. E., III; Laughton, C. A.; Orozco, M. Refinement of the Amber Force Field for Nucleic Acids: Improving the Description of α/γ Conformers. *Biophys. J.* **2007**, *92*, 3817−3829.
(42) Mazur, A. K. Evaluation of Elastic Properties of Atomistic DNA Models. *Biophys. J.* **2006**, *91*, 4507−4518.
(43) Sponer, J.; Jurecka, P.; Marchan, I.; Luque, J.; Orozco, M.; Hobza, P. Nature of Base Stacking: Reference Quantum-Chemical Stacking Energies in Ten Unique B-DNA Base-Pair Steps. *Chem.—Eur. J.* **2006**, *12*, 2854−2865.
(44) Kuznetsov, S. V.; Sugimura, S.; Vivas, P.; Crothers, D. M.; Ansari, A. Direct Observation of DNA Bending/Unbending Kinetics in Complex with DNA-Bending Protein IHF. *Proc. Natl. Acad. Sci. U.S.A.* **2006**, *103*, 18515−18520.
(45) Vivas, P.; Kuznetsov, S. V.; Ansari, A. New Insights into the Transition Pathway from Nonspecific to Specific Complex of DNA with *Escherichia coli* Integration Host Factor. *J. Phys. Chem. B* **2008**, *112*, 5997−6007.
(46) Vivas, P.; Velmurugu, Y.; Kuznetsov, S. V.; Rice, P. A.; Ansari, A. Mapping the Transition State for DNA Bending by IHF. *J. Mol. Biol.* **2012**, *418*, 300−315.
(47) Mathew-Fenn, R. S.; Das, R.; Harbury, P. A. B. Remeasuring the Double Helix. *Science* **2008**, *322*, 446−449.